



Published in final edited form as:

Gastroenterology. 2011 October ; 141(4): 1371–1380.e2. doi:10.1053/j.gastro.2011.06.071.

Disruption of the Mouse Protein Tyrosine Kinase 6 Gene Prevents STAT3 Activation and Confers Resistance to Azoxymethane

Jessica Gierut¹, Yu Zheng¹, Wenjun Bie¹, Robert E. Carroll², Susan Ball-Kell³, Andrea Haegerbarth^{1,4}, and Angela L. Tyner^{1,2,*}

¹Department of Biochemistry and Molecular Genetics, University of Illinois at Chicago, Chicago, IL 60607

²Department of Medicine, University of Illinois at Chicago, Chicago, IL 60607

³University of Illinois College of Veterinary Medicine Veterinary Diagnostic Laboratory Urbana, IL 61802

Abstract

Background & Aims—Protein tyrosine kinase 6 (PTK6) is expressed throughout the gastrointestinal tract and is a negative regulator of proliferation that promotes differentiation and DNA-damage induced apoptosis in the small intestine. PTK6 is not expressed in normal mammary gland, but is induced in most human breast tumors. Signal transducer and activator of transcription 3 (STAT3) mediates pathogenesis of colon cancer and is a substrate of PTK6. We investigated the role of PTK6 in colon tumorigenesis.

Methods—*Ptk6* *+/+* and *Ptk6* *-/-* mice were injected with azoxymethane alone or in combination with dextran sodium sulfate; formation of aberrant crypt foci (ACF) and colon tumors was examined. Effects of disruption of *Ptk6* on proliferation, apoptosis, and STAT3 activation were examined by immunoblot and immunohistochemical analyses. Regulation of STAT3 activation was examined in the HCT116 colon cancer cell line and young adult mouse colon (YAMC) cells.

Results—*Ptk6* *-/-* mice developed fewer azoxymethane-induced ACF and tumors. Induction of PTK6 increased apoptosis, proliferation, and STAT3 activation in *Ptk6* *+/+* mice injected with azoxymethane. Disruption of *Ptk6* impaired STAT3 activation following azoxymethane injection, and reduced active STAT3 levels in *Ptk6* *-/-* tumors. Stable knockdown of PTK6 reduced basal

© 2011 The American Gastroenterological Association. Published by Elsevier Inc. All rights reserved.

*Corresponding author: University of Illinois College of Medicine, Department of Biochemistry and Molecular Genetics, M/C 669, 900 South Ashland Avenue, Chicago, Illinois 60607, Phone: 312-996-7964, Fax: 312-413-4892, atyner@uic.edu.

⁴Current Address: Bayer Schering Pharma AG, GDD, TCR in vivo 3, Berlin, Germany

The authors have no conflict of interest to report.

Author Contributions: Gierut: Acquisition of data, analysis and interpretation of data, drafting of the manuscript; Zheng: Acquisition of data, analysis and interpretation of data; Bie: Acquisition of data, analysis and interpretation of data; Carroll: Acquisition of data, analysis and interpretation of data; Ball-Kell: Acquisition of data, analysis and interpretation of data; Haegerbarth: Acquisition of data, analysis and interpretation of data; Tyner: study concept and design, analysis and interpretation of data, drafting of the manuscript, obtained funding, study supervision.

Publisher's Disclaimer: This is a PDF file of an unedited manuscript that has been accepted for publication. As a service to our customers we are providing this early version of the manuscript. The manuscript will undergo copyediting, typesetting, and review of the resulting proof before it is published in its final citable form. Please note that during the production process errors may be discovered which could affect the content, and all legal disclaimers that apply to the journal pertain.

levels of active STAT3, as well as activation of STAT3 by epidermal growth factor in HCT116 cells. Disruption of *Ptk6* reduced activity of STAT3 in YAMC cells.

Conclusions—PTK6 promotes STAT3 activation in the colon following injection of the carcinogen azoxymethane and regulates STAT3 activity in mouse colon tumors and in the HCT116 and YAMC cell lines. Disruption of *Ptk6* decreases azoxymethane-induced colon tumorigenesis in mice.

Keywords

BRK; cancer cell signaling; neoplasm; tumor formation; EGF; Sik; AOM; colon cancer; STAT3

INTRODUCTION

Protein tyrosine kinase 6 (PTK6; also called BRK for breast tumor kinase) belongs to a family of intracellular tyrosine kinases related to but distinct from the Src family [reviewed in ¹⁻³]. It is expressed in normal epithelial cells of the gastrointestinal tract ⁴⁻⁷. Disruption of the mouse *Ptk6* gene resulted in increased epithelial cell proliferation, villus length and crypt depth, and enhanced levels of nuclear β -catenin in crypt cells in the small intestine. Maturation of enterocytes was delayed in *Ptk6*^{-/-} mice ⁸. Recently, we showed that PTK6 associates with β -catenin and negatively regulates β -catenin/TCF transcriptional activity ⁹. Knockdown of PTK6 in the SW620 colon cancer cell line led to an increase in β -catenin/TCF transcriptional activity and increased expression of β -catenin/TCF target genes. *Ptk6*^{-/-} mice displayed increased expression of a β -catenin/TCF regulated reporter in the mouse gastrointestinal tract ⁹, providing additional evidence that *Ptk6* can act as an inhibitor of β -catenin/TCF transcription in vivo.

Alterations in PTK6 expression and/or localization influence its functions. Although normally expressed in nondividing differentiated epithelial cells in the intestine, we found that PTK6 is induced in mouse small intestinal crypt epithelial cells following total body γ irradiation¹⁰. Induction of PTK6 in proliferating progenitor cells following DNA damage led to increased apoptosis and inhibition of prosurvival signaling ¹⁰. PTK6 is not expressed in normal mammary gland or ovary, but is detected in breast tumors ¹¹⁻¹⁴ and high-grade ovarian carcinomas ¹⁵. In breast cancer cells, PTK6 promotes activation of signaling pathways that promote oncogenesis [reviewed in ^{1,2}]. In normal prostate, PTK6 is expressed in nuclei of luminal epithelial cells, but is relocalized to the cytoplasm in prostate tumors ¹⁶. Recently we determined that cytoplasmic PTK6 has growth promoting functions in prostate cancer cells ¹⁷, and is able to directly phosphorylate and promote AKT activation in response to EGF ¹⁸.

Signal transducers and activators of transcription (STATs) regulate many fundamental biological processes, such as proliferation, cell survival, angiogenesis and the immune response ¹⁹. PTK6 enhances activating tyrosine phosphorylation of STAT3 ²⁰ and STAT5a and 5b ²¹ in cell lines. PTK6 also phosphorylates the adaptor protein STAP2 ²², which plays a role in STAT3 activation ^{23,24}. Activated STAT3 has been implicated in many types of cancer, including colorectal cancer ^{25,26}.

Colorectal cancer is the second leading cause of cancer-related deaths in the United States ²⁷. Given that PTK6 promotes both differentiation ⁸ and apoptosis ¹⁰ in the mouse small intestine, we initially hypothesized that PTK6 might have tumor suppressor functions in the colon. However, we found that *Ptk6*^{-/-} mice are resistant to the colon carcinogen azoxymethane (AOM) when compared with wild type counterparts. Resistance to AOM correlates with impaired STAT3 activation and reduced expression of STAT3 targets in *Ptk6*^{-/-} mice. Although PTK6 regulates growth suppression and differentiation in the normal

intestine, our data indicate that PTK6 is able to promote STAT3 activation and development of colorectal cancers in vivo.

MATERIALS AND METHODS

Animals and Tissues

The B6.129SV-*Ptk6*^{tm1Aty} 2.8 mouse line was previously described⁸. The 11.6 line was generated like the 2.8 line from an independent ES cell clone. B6.129SV mice were backcrossed with inbred C57BL6/J (B6) mice for more than twelve generations to generate *Ptk6*^{+/+} and *Ptk6*^{-/-} in the B6 background. Sex and age matched B6.129SV or B6 mice were analyzed in different experiments as indicated.

For apoptosis and proliferation studies, *Ptk6*^{+/+} and *Ptk6*^{-/-} B6.129SV mice were injected with 15 mg/kg of AOM and sacrificed 6 or 72 hours later. In the AOM/DSS combination model *Ptk6*^{+/+} and *Ptk6*^{-/-} B6 mice were given a single injection of AOM (10 mg/kg), and one week after injection, animals received 2% DSS in their drinking water for 7 days²⁸. Animals were sacrificed at 20 weeks. In the AOM colon tumorigenesis model *Ptk6*^{+/+} and *Ptk6*^{-/-} B6 mice were injected with AOM (10 mg/kg) once a week for 6 consecutive weeks and sacrificed at the end of 39 weeks. Colon tissues were fixed in 4% paraformaldehyde. Protein lysates were prepared from distal colon as previously described⁸.

Cell Culture

HCT116 cells (ATCC CCL-247) were cultured in Dulbecco's modified Eagle medium (DMEM) containing 10% fetal bovine serum. Cells were serum starved for 48 hours and stimulated with EGF (25 ng/ml). Immortalized young adult mouse colon (YAMC) epithelial cells were a gift from Robert Whitehead (Vanderbilt University Medical Center, Nashville, TN)²⁹. *Ptk6*^{-/-} YAMC cells have been described³⁰. Control YAMC and *Ptk6*^{-/-} YAMC cells were grown with INF- γ (5 U/ml) at 33°C in RPMI 1640 medium supplemented with 10% fetal bovine serum. *Ptk6*^{-/-} YAMC cells were dissociated with Cellstripper (Mediatech Inc, Manassas, VA).

Immunoblotting and Antibodies

Immunoblotting was performed as described⁸, using anti-human PTK6 (C-18, G-6), anti-mouse PTK6 (C-17) (Santa Cruz Biotechnology, Inc., Santa Cruz, CA); cleaved-Caspase-3, phospho-STAT3 (Tyr705), STAT3 (9132) and Bcl-xL (54H6) (Cell Signaling Technology, Beverly, MA); β -actin (Sigma-Aldrich, St. Louis, MO); anti-Heat Shock Protein 70 (clone 3A3, Millipore, Billerica, MA); and anti-Cyclin D1 (DCS 6, Thermo Fisher Scientific Inc., Fremont, CA). Secondary antibodies (donkey anti-rabbit or sheep anti-mouse conjugated to horseradish peroxidase, Amersham Biosciences, Piscataway, NJ) were detected by chemiluminescence with SuperSignal[®] West Dura Extended Duration Substrate (Pierce, Rockford, IL).

Identification of ACF

Mice at 6–8 weeks of age were subjected to weekly injections of AOM (10 mg/kg) in sterile saline for 6 weeks and sacrificed 4 weeks after the last injection. Whole mount colons were fixed in 70% EtOH and stained with methylene blue. Total numbers of ACF were counted independently in a blinded fashion by two individuals using light microscopy³¹.

Immunohistochemistry

Immunohistochemistry was performed using anti-cleaved-Caspase-3 (Cell Signaling Technology) and the Vectastain ABC Kit (Vector Laboratories, Burlingame, CA) according

to manufacturer's instructions. Reactions were visualized with FITC-Avidin DCS (Vector Laboratories). Nuclei were stained with 4',6-diamidino-2-phenylindole (DAPI). Immunohistochemistry was performed with anti-PTK6 (C-17, Santa Cruz Biotechnology), STAT3 and P-Y705-STAT3 antibodies (Cell Signaling Technology). Tyramide amplification (TSA™ Biotin System, PerkinElmer, Waltham, MA) was performed to detect P-Y705 STAT3 according to manufacturer's instructions. Reactions were visualized with 3,3'-diaminobenzidine (DAB) and in some cases counterstained with hematoxylin. Controls were performed with normal rabbit or normal mouse serum.

PTK6 Knockdown in HCT116 Cells

The MISSION TRC shRNA Target Set directed against PTK6 was purchased from Sigma-Aldrich. Lentiviruses expressing TRCN0000021459 (shRNA49), TRCN0000021552 (shRNA52) and empty vector were produced in the HEK293FT packaging cell line by co-transfection with compatible packaging plasmids HIV trans and VSVG³². HCT116 cells were infected and placed in selection medium containing 1 µg/ml puromycin for 2 weeks.

Statistics

Quantitative analyses were performed using the NIH Image J program³³. Results are shown as the mean ± SD. P-values were determined using the 2-tailed Student's T test (Microsoft Excel, 2004). A difference was considered statistically significant if the P-value was equal to or less than 0.05.

RESULTS

Disruption of the *Ptk6* gene reduces ACF formation in vivo

To examine contributions of PTK6 to colon cancer, wild type and *Ptk6*^{-/-} mice were treated with the carcinogen AOM that induces aberrant crypt foci (ACF) and colon tumors in rodents³⁴. ACF are abnormally large raised colonic crypts that are proposed precursors of colorectal carcinoma [reviewed in³⁵] that can be visualized by methylene blue staining of whole mount colons. We examined ACF formation in two independently derived lines of *Ptk6*^{-/-} mice, termed 2.8 and 11.6. Wild type and *Ptk6*^{-/-} mice were subjected to weekly injections of AOM for 6 weeks and sacrificed 4 weeks after the last injection. Typical ACF are shown in Figure 1A. We found that wild type mice exhibited a significantly higher incidence of ACF formation compared with *Ptk6*^{-/-} mice (Figure 1B). Colons of both *Ptk6*^{+/+} and *Ptk6*^{-/-} mice that were subjected to AOM were divided into 1 cm sections from the proximal (cecum) to distal (rectum) end, and the number of ACF per cm was recorded. Most ACF formed in the distal 3 cm of the colon (Figure 1C). The B6.129SV 2.8 and 11.6 lines of *Ptk6*^{-/-} mice were both resistant to ACF formation.

Ptk6^{-/-} mice are resistant to AOM induced tumorigenesis

Treatment with AOM and dextran sodium sulfate (DSS), which induces injury and inflammation and acts as a tumor promoter, leads to rapid development of adenocarcinomas in the mouse colon²⁸. To determine consequences of disruption of the *Ptk6* gene on AOM-DSS induced tumor formation, age-matched wild type and *Ptk6*^{-/-} mice were given a single intraperitoneal injection of AOM and then 2% DSS in their drinking water for one week, followed by monitoring for 20 weeks (Figure 2A). Wild type mice showed higher mortality and morbidity upon treatment with a loss of 50% of treated mice. *Ptk6*^{-/-} mice showed 80% survival and lower morbidity upon treatment compared with wild type controls (Figure 2B). Wild type and *Ptk6*^{-/-} mice that survived until the end of the 20-week study were sacrificed and whole mount colons were examined from the proximal to distal end (cecum to rectum) using light microscopy. Large nodular and polyploid colonic tumors were

observed in the distal halves of the colons of wild type mice, corresponding to the region that developed the most ACF. The number and size of tumors were substantially reduced in *Ptk6*^{-/-} mice when compared with control wild type mice (Figure 2C; Supplemental Figure S1A). Tumors that formed in the wild type animals displayed high-grade dysplasia with some areas consistent with intramucosal carcinoma. In contrast, most adenomas that developed in *Ptk6* null mice displayed low-grade dysplasia (Figure 2D).

While C57BL/6J mice are resistant to tumor development induced by AOM alone, we also injected B6 *Ptk6*^{+/+} and *Ptk6*^{-/-} mice with AOM for 6 consecutive weeks and then sacrificed mice at 39 weeks. We discovered greater numbers of tumors in wild type mice than in *Ptk6*^{-/-} mice (Supplemental data, Figure S1B). This suggests that PTK6 does not require DSS treatment and a strong inflammatory environment to promote tumorigenesis.

PTK6 expression is induced in colonic crypts after AOM treatment and promotes apoptosis and compensatory proliferation

PTK6 expression is induced in small intestinal crypts following irradiation, where it is required for efficient DNA-damage induced apoptosis¹⁰. To begin to understand the role of PTK6 following AOM induced DNA damage, PTK6 expression and localization were examined in untreated and AOM treated B6.129SV wild type mice using immunohistochemistry. Consistent with previous data⁸, PTK6 protein expression was largely confined to non-proliferative differentiated cells at the surface epithelium of the colon in untreated mice (Figure 3A, 0 h). However, following AOM treatment, PTK6 expression was induced in the crypts, with strong expression localized to single cells within the proliferative zone (Fig 3A, 6 h and 72 h).

Deregulation of apoptosis and/or proliferation may contribute to the development of cancer³⁶. AOM regulates apoptosis and proliferation, with apoptosis occurring between 4 and 8 hours and peak proliferation around 72 hours following a single injection of AOM in rodents³⁷. To examine the role that PTK6 plays in AOM induced apoptosis, *Ptk6*^{+/+} and *Ptk6*^{-/-} B6 mice were sacrificed at 6 and 72 hours post AOM injection. Immunohistochemistry for cleaved Caspase-3 revealed little spontaneous apoptosis in untreated colons of wild type and *Ptk6*^{-/-} mice. However, a significant increase in apoptosis was detected in *Ptk6*^{+/+} mice compared with *Ptk6*^{-/-} mice at the 6-hour time point following AOM treatment (Figure 3B and C). These data are consistent with prior reports that PTK6 expression plays an important role in DNA damage-induced apoptosis in the small intestinal epithelium¹⁰. Immunoblotting also revealed higher levels of cleaved Caspase-3 at 6 hours post AOM injection in wild type mice (Figure 3D).

To determine if PTK6 expression has an effect on proliferation *Ptk6*^{+/+} and *Ptk6*^{-/-} B6.129SV mice were subjected to a single injection of AOM and sacrificed 6 and 72 hours post injection. Two hours prior to sacrifice, mice were injected with bromodeoxyuridine (BrdU) and proliferative cells were identified using a BrdU monoclonal antibody (Fig 3E and F). Comparable levels of proliferation were detected in untreated wild type and *Ptk6*^{-/-} mice (Fig 3E, 0 h). However, a significant increase in proliferation was detected in wild type mice compared with *Ptk6*^{-/-} mice at the 6-hour time point post AOM injection (Figure 3F).

Disruption of *Ptk6* impairs activation of STAT3 in vivo and in vitro

To identify signaling pathways downstream of PTK6, we examined expression and activation of AKT, ERK1/2 and STAT3. In the mouse small intestine, we previously showed that PTK6 negatively regulates AKT and ERK1/2 activity after irradiation, but we were unable to detect differences in activation of these signaling proteins in wild type and *Ptk6*^{-/-} colons after AOM injection. STAT3 activation has been linked to colon

tumorigenesis^{25, 26}, and PTK6 was shown to phosphorylate and activate STAT3 in cell lines²⁰. In untreated *Ptk6* *+/+* and *Ptk6* *-/-* mice, we saw comparable levels of total and phospho-STAT3. However, at 6 and 72 h post AOM administration, we detected pronounced STAT3 activation only in wild type mice (Figure 4A and B) by examining phosphorylation of STAT3 tyrosine residue 705 (P-STAT3). A corresponding increase in expression of proteins encoded by genes that are activated by STAT3, including Bcl-xL³⁸, Hsp70³⁹, and Cyclin D1⁴⁰ was detected in lysates isolated from wild type colons after AOM treatment (Figure 4A, Supplemental Figure S3).

Disruption of *Ptk6* impaired STAT3 activation after AOM administration, and basal levels of tyrosine phosphorylated STAT3 were not maintained in *Ptk6* *-/-* mice, relative to levels at the 0 h timepoint (Figure 4A and B). Decreased levels of active P-STAT3 were also detected in *Ptk6* *-/-* mice at 6 h post AOM injection using immunohistochemistry (Figure 4C). At later times, P-STAT3 levels were reduced in the AOM/DSS induced tumors that developed in *Ptk6* *-/-* mice shown in Figure 2 (Figure 4D). Following AOM-induced DNA damage, PTK6 promotes activation of STAT3 by tyrosine phosphorylation in wild type mice. The significant reduction in STAT3 activation after AOM administration and in established tumors may account for the reduced tumor burden in *Ptk6* *-/-* mice. These data suggest a non-redundant role for PTK6 in regulating STAT3 activity.

The colon is a complex tissue and the colonic epithelial cells receive signals from a variety of neighboring cell types including mesenchymal cells and inflammatory cells. To determine if PTK6 is able to regulate STAT3 activation in an epithelial cell autonomous manner, we turned to the HCT116 colon cancer epithelial cell line that expresses moderate levels of endogenous PTK6. Lysates were prepared from selected stable pools of HCT116 cells containing the lentiviral vector control or one of two different shRNAs that target PTK6 (shRNA49 and shRNA52), and total STAT3 and P-STAT3 levels were examined by immunoblotting. Baseline levels of P-STAT3 are higher in the vector control stable cell lines than in stable cell lines with knockdown of PTK6, indicating that PTK6 expression contributes to constitutive activation of STAT3 in HCT116 cells (Figure 5A, B). Each of the stable pools was also serum starved for 48 hours and then stimulated with EGF for 2, 5 and 10 minutes. Phosphorylation of STAT3 is evident by two minutes post EGF addition in the vector control cells, but not in the *Ptk6* knockdown cells (Figure 5C, D), demonstrating that PTK6 is required for EGF induced activation of STAT3.

We also examined STAT3 activation and PTK6 expression in immortalized young adult mouse colon (YAMC) cells isolated from wild type and *Ptk6* *-/-* mice³⁰. Higher levels of P-STAT3 and proteins encoded by genes activated by STAT3, including Bcl-xL and Cyclin D1 were detected in lysates from wild type YAMC cells compared with *Ptk6* *-/-* YAMC cells (Figure 5E and F). In general, the level of STAT3 activation correlates well with PTK6 expression, underscoring a role for PTK6 in regulating STAT3 activation in colon cells.

DISCUSSION

PTK6 is not expressed in the normal mammary gland, but is expressed in a majority of breast tumors [reviewed in^{1, 2}]. In contrast, PTK6 is expressed in the normal linings of the gastrointestinal tract and skin, where it is primarily localized to nondividing differentiated epithelial cells⁵. Disruption of mouse *Ptk6* revealed that it plays roles promoting growth arrest and maturation of columnar epithelial cells in the small intestine⁸. In addition, PTK6 expression is induced in small intestinal crypts after DNA damage, where it inhibits prosurvival signaling and promotes apoptosis. Enhanced apoptosis was accompanied by increased compensatory cell proliferation that could counteract the loss of cells to maintain normal tissue homeostasis¹⁰. Similar to the response to γ -irradiation in the small

intestine¹⁰, PTK6 expression was induced, and apoptosis and proliferation were enhanced in colons of wild type mice compared with *Ptk6*^{-/-} mice following injection of the DNA-damaging agent AOM (Figure 3). Here we demonstrate that PTK6 contributes to colon tumorigenesis in the AOM/DSS and AOM mouse models of colon cancer.

STAT3 plays a critical role regulating proliferation, survival, migration, and inflammation¹⁹. Epithelial STAT3 plays essential roles in the initiation and progression of skin cancer^{41, 42}, pancreatic ductal adenocarcinoma^{43, 44} and colitis associated colon cancer^{25, 26}. Disruption of *Stat3* specifically in intestinal epithelial cells compromised proliferation in response to DSS alone and in the AOM/DSS tumorigenesis model²⁶. We found that disruption of the *Ptk6* gene impaired activation of STAT3 following AOM administration. By six hours post AOM injection, we see induction of PTK6 in distal colonic crypts, increased apoptosis and proliferation in wild type mice (Figure 3). We show that PTK6 regulates activating tyrosine phosphorylation of STAT3 in the colon after AOM induced DNA damage, providing the first evidence that PTK6 controls STAT3 activation in vivo (Figure 4). Increased STAT3 activation would enhance survival and promote expansion of cells bearing mutations. Our in vivo data suggest that in addition to its role in tumor initiation, PTK6 also regulates STAT3 activation in established tumors (Figure 4D).

STAT3 is constitutively active in many human cancers and tumor cell lines⁴⁵, including the HCT116 human colon adenocarcinoma cell line (Figure 5). PTK6 plays a critical role maintaining constitutive activation of STAT3 in the HCT116 colon cancer cell line, and is important for modulating the response of these cells to EGF. Interestingly, EGF receptor (EGFR) signaling contributes to tumor progression in the mouse AOM model⁴⁶, and the ability of EGFR to activate STAT3 signaling would be impaired in the *Ptk6*^{-/-} mice. Basal levels of STAT3 activation were also reduced in *Ptk6*^{-/-} YAMC cells compared with wild type control YAMC cells (Figure 5E, F).

Previously, we demonstrated that nuclear PTK6 inhibits β -catenin/TCF transcription⁹. To determine if disruption of *Ptk6* has an impact on tumorigenesis in *Apc*^{Min+} mice that display increased β -catenin/TCF transcriptional activity⁴⁷, *Ptk6*^{-/-} mice were crossed with *Apc*^{Min+} mice to generate *Ptk6*^{+/+} and *Ptk6*^{-/-} *Apc*^{Min+} animals. Disruption of *Ptk6* did not significantly impact survival or tumor formation in *Apc*^{Min+} mice (Figure S2). Intestinal cancers are believed to originate from crypt stem cells⁴⁸, and PTK6 is normally expressed in differentiated nondividing epithelial cells where it would not be able to contribute to tumor initiation. However, PTK6 is induced in intestinal crypts after DNA damage caused by the administration of AOM (Figure 3A) or γ -irradiation¹⁰. It is possible that disruption of *Ptk6* might have a more profound impact on tumor growth in *Apc*^{Min+} mice following DNA damage induced by repetitive administration of chemotherapeutic drugs or radiation.

PTK6 has context dependent functions that differ depending on the cell type in which it is expressed, its intracellular localization, and expression levels. Although it has growth inhibiting and differentiating promoting functions in normal epithelia, induction of PTK6 in crypt epithelial cells stimulates apoptosis of injured cells, while it also promotes proliferation and tumorigenesis through activation of STAT3. These studies are the first to highlight a role for PTK6 in the etiology of colon cancer. As an activator of STAT3, PTK6 is a potential therapeutic target in colon cancer, and consequences of disrupting PTK6 in established colon tumors merits further investigation.

Supplementary Material

Refer to Web version on PubMed Central for supplementary material.

Acknowledgments

Funding: This work was supported by NIH Grant DK44525 (A.L.T.). J.J.G. received support from a NRSA/NIH Institutional T32 training grant DK07739, and an AGA Foundation Graduate Student Research Fellowship Award.

References

1. Brauer PM, Tyner AL. Building a better understanding of the intracellular tyrosine kinase PTK6 - BRK by BRK. *Biochim Biophys Acta*. 2010; 1806:66–73. [PubMed: 20193745]
2. Ostrander JH, Daniel AR, Lange CA. Brk/PTK6 signaling in normal and cancer cell models. *Curr Opin Pharmacol*. 2010
3. Serfas MS, Tyner AL. Brk, Srm, Frk, and Src42A form a distinct family of intracellular Src-like tyrosine kinases. *Oncol Res*. 2003; 13:409–19. [PubMed: 12725532]
4. Siyanova EY, Serfas MS, Mazo IA, Tyner AL. Tyrosine kinase gene expression in the mouse small intestine. *Oncogene*. 1994; 9:2053–7. [PubMed: 8208550]
5. Vasioukhin V, Serfas MS, Siyanova EY, Polonskaia M, Costigan VJ, Liu B, Thomason A, Tyner AL. A novel intracellular epithelial cell tyrosine kinase is expressed in the skin and gastrointestinal tract. *Oncogene*. 1995; 10:349–57. [PubMed: 7838533]
6. Llor X, Serfas MS, Bie W, Vasioukhin V, Polonskaia M, Derry J, Abbott CM, Tyner AL. BRK/Sik expression in the gastrointestinal tract and in colon tumors. *Clin Cancer Res*. 1999; 5:1767–77. [PubMed: 10430081]
7. Haegerbarth A, Heap D, Bie W, Derry JJ, Richard S, Tyner AL. The nuclear tyrosine kinase BRK/Sik phosphorylates and inhibits the RNA-binding activities of the Sam68-like mammalian proteins SLM-1 and SLM-2. *J Biol Chem*. 2004; 279:54398–404. [PubMed: 15471878]
8. Haegerbarth A, Bie W, Yang R, Crawford SE, Vasioukhin V, Fuchs E, Tyner AL. Protein tyrosine kinase 6 negatively regulates growth and promotes enterocyte differentiation in the small intestine. *Mol Cell Biol*. 2006; 26:4949–57. [PubMed: 16782882]
9. Palka-Hamblin HL, Gierut JJ, Bie W, Brauer PM, Zheng Y, Asara JM, Tyner AL. Identification of beta-catenin as a target of the intracellular tyrosine kinase PTK6. *J Cell Sci*. 2010; 123:236–45. [PubMed: 20026641]
10. Haegerbarth A, Perekatt AO, Bie W, Gierut JJ, Tyner AL. Induction of protein tyrosine kinase 6 in mouse intestinal crypt epithelial cells promotes DNA damage-induced apoptosis. *Gastroenterology*. 2009; 137:945–54. [PubMed: 19501589]
11. Barker KT, Jackson LE, Crompton MR. BRK tyrosine kinase expression in a high proportion of human breast carcinomas. *Oncogene*. 1997; 15:799–805. [PubMed: 9266966]
12. Ostrander JH, Daniel AR, Lofgren K, Kleer CG, Lange CA. Breast tumor kinase (protein tyrosine kinase 6) regulates heregulin-induced activation of ERK5 and p38 MAP kinases in breast cancer cells. *Cancer Res*. 2007; 67:4199–209. [PubMed: 17483331]
13. Xiang B, Chatti K, Qiu H, Lakshmi B, Krasnitz A, Hicks J, Yu M, Miller WT, Muthuswamy SK. Brk is coamplified with ErbB2 to promote proliferation in breast cancer. *Proc Natl Acad Sci U S A*. 2008; 105:12463–8. [PubMed: 18719096]
14. Irie HY, Shrestha Y, Selfors LM, Frye F, Iida N, Wang Z, Zou L, Yao J, Lu Y, Epstein CB, Natesan S, Richardson AL, Polyak K, Mills GB, Hahn WC, Brugge JS. PTK6 regulates IGF-1-induced anchorage-independent survival. *PLoS One*. 2010; 5:e11729. [PubMed: 20668531]
15. Schmandt RE, Bennett M, Clifford S, Thornton A, Jiang F, Broaddus RR, Sun CC, Lu KH, Sood AK, Gershenson DM. The BRK Tyrosine Kinase is Expressed in High-Grade Serous Carcinoma of the Ovary. *Cancer Biol Ther*. 2006;5.
16. Derry JJ, Prins GS, Ray V, Tyner AL. Altered localization and activity of the intracellular tyrosine kinase BRK/Sik in prostate tumor cells. *Oncogene*. 2003; 22:4212–20. [PubMed: 12833144]
17. Brauer PM, Zheng Y, Wang L, Tyner AL. Cytoplasmic retention of protein tyrosine kinase 6 promotes growth of prostate tumor cells. *Cell Cycle*. 2010; 9:4190–4199. [PubMed: 20953141]
18. Zheng Y, Peng M, Wang Z, Asara JM, Tyner AL. Protein tyrosine kinase 6 directly phosphorylates AKT and promotes AKT activation in response to epidermal growth factor. *Mol Cell Biol*. 2010; 30:4280–92. [PubMed: 20606012]

19. Yu H, Pardoll D, Jove R. STATs in cancer inflammation and immunity: a leading role for STAT3. *Nat Rev Cancer*. 2009; 9:798–809. [PubMed: 19851315]
20. Liu L, Gao Y, Qiu H, Miller WT, Poli V, Reich NC. Identification of STAT3 as a specific substrate of breast tumor kinase. *Oncogene*. 2006; 25:4904–12. [PubMed: 16568091]
21. Weaver AM, Silva CM. Signal transducer and activator of transcription 5b: a new target of breast tumor kinase/protein tyrosine kinase 6. *Breast Cancer Res*. 2007; 9:R79. [PubMed: 17997837]
22. Mitchell PJ, Sara EA, Crompton MR. A novel adaptor-like protein which is a substrate for the non-receptor tyrosine kinase, BRK. *Oncogene*. 2000; 19:4273–82. [PubMed: 10980601]
23. Ikeda O, Miyasaka Y, Sekine Y, Mizushima A, Muromoto R, Nanbo A, Yoshimura A, Matsuda T. STAP-2 is phosphorylated at tyrosine-250 by Brk and modulates Brk-mediated STAT3 activation. *Biochem Biophys Res Commun*. 2009; 384:71–5. [PubMed: 19393627]
24. Ikeda O, Sekine Y, Mizushima A, Nakasuji M, Miyasaka Y, Yamamoto C, Muromoto R, Nanbo A, Oritani K, Yoshimura A, Matsuda T. Interactions of STAP-2 with Brk and STAT3 participate in cell growth of human breast cancer cells. *J Biol Chem*. 2010
25. Grivennikov S, Karin E, Terzic J, Mucida D, Yu GY, Vallabhapurapu S, Scheller J, Rose-John S, Cheroutre H, Eckmann L, Karin M. IL-6 and Stat3 are required for survival of intestinal epithelial cells and development of colitis-associated cancer. *Cancer Cell*. 2009; 15:103–13. [PubMed: 19185845]
26. Bollrath J, Pheesse TJ, von Burstin VA, Putoczki T, Bennecke M, Bateman T, Nebelsiek T, Lundgren-May T, Canli O, Schwitalla S, Matthews V, Schmid RM, Kirchner T, Arkan MC, Ernst M, Greten FR. gp130-mediated Stat3 activation in enterocytes regulates cell survival and cell-cycle progression during colitis-associated tumorigenesis. *Cancer Cell*. 2009; 15:91–102. [PubMed: 19185844]
27. ACS. American Cancer Society's Guide to Colorectal Cancer. 2011. <http://www.cancer.org/Cancer/ColonandRectumCancer/DetailedGuide/index>
28. Tanaka T, Kohno H, Suzuki R, Yamada Y, Sugie S, Mori H. A novel inflammation-related mouse colon carcinogenesis model induced by azoxymethane and dextran sodium sulfate. *Cancer Sci*. 2003; 94:965–73. [PubMed: 14611673]
29. Whitehead RH, VanEeden PE, Noble MD, Ataliotis P, Jat PS. Establishment of conditionally immortalized epithelial cell lines from both colon and small intestine of adult H-2Kb-tsA58 transgenic mice. *Proc Natl Acad Sci U S A*. 1993; 90:587–91. [PubMed: 7678459]
30. Whitehead RH, Robinson PS, Williams JA, Bie W, Tyner AL, Franklin JL. Conditionally immortalized colonic epithelial cell line from a Ptk6 null mouse that polarizes and differentiates in vitro. *J Gastroenterol Hepatol*. 2008
31. Pretlow TP, Pretlow TG. Mutant KRAS in aberrant crypt foci (ACF): initiation of colorectal cancer? *Biochim Biophys Acta*. 2005; 1756:83–96. [PubMed: 16219426]
32. Feng Z, Cerveny M, Yan Z, He B. The VP35 protein of Ebola virus inhibits the antiviral effect mediated by double-stranded RNA-dependent protein kinase PKR. *J Virol*. 2007; 81:182–92. [PubMed: 17065211]
33. Rasband, WS. ImageJ. U. S. National Institutes of Health; Bethesda, Maryland, USA: 1997–2011. <http://imagej.nih.gov/ij/>
34. Bird RP. Observation and quantification of aberrant crypts in the murine colon treated with a colon carcinogen: preliminary findings. *Cancer Lett*. 1987; 37:147–51. [PubMed: 3677050]
35. Khare S, Chaudhary K, Bissonnette M, Carroll R. Aberrant crypt foci in colon cancer epidemiology. *Methods Mol Biol*. 2009; 472:373–86. [PubMed: 19107443]
36. Green DR, Evan GI. A matter of life and death. *Cancer Cell*. 2002; 1:19–30. [PubMed: 12086884]
37. Hirose Y, Yoshimi N, Makita H, Hara A, Tanaka T, Mori H. Early alterations of apoptosis and cell proliferation in azoxymethane-initiated rat colonic epithelium. *Jpn J Cancer Res*. 1996; 87:575–82. [PubMed: 8766520]
38. Shen Y, Devgan G, Darnell JE Jr, Bromberg JF. Constitutively activated Stat3 protects fibroblasts from serum withdrawal and UV-induced apoptosis and antagonizes the proapoptotic effects of activated Stat1. *Proc Natl Acad Sci U S A*. 2001; 98:1543–8. [PubMed: 11171987]

39. Yamagishi N, Fujii H, Saito Y, Hatayama T. Hsp105beta upregulates hsp70 gene expression through signal transducer and activator of transcription-3. *Febs J.* 2009; 276:5870–80. [PubMed: 19754877]
40. Leslie K, Lang C, Devgan G, Azare J, Berishaj M, Gerald W, Kim YB, Paz K, Darnell JE, Albanese C, Sakamaki T, Pestell R, Bromberg J. Cyclin D1 is transcriptionally regulated by and required for transformation by activated signal transducer and activator of transcription 3. *Cancer Res.* 2006; 66:2544–52. [PubMed: 16510571]
41. Chan KS, Sano S, Kiguchi K, Anders J, Komazawa N, Takeda J, DiGiovanni J. Disruption of Stat3 reveals a critical role in both the initiation and the promotion stages of epithelial carcinogenesis. *J Clin Invest.* 2004; 114:720–8. [PubMed: 15343391]
42. Kataoka K, Kim DJ, Carbajal S, Clifford JL, DiGiovanni J. Stage-specific disruption of Stat3 demonstrates a direct requirement during both the initiation and promotion stages of mouse skin tumorigenesis. *Carcinogenesis.* 2008; 29:1108–14. [PubMed: 18453544]
43. Fukuda A, Wang SC, Morris JPt, Folias AE, Liou A, Kim GE, Akira S, Boucher KM, Firpo MA, Mulvihill SJ, Hebrok M. Stat3 and MMP7 contribute to pancreatic ductal adenocarcinoma initiation and progression. *Cancer Cell.* 2011; 19:441–55. [PubMed: 21481787]
44. Lesina M, Kurkowski MU, Ludes K, Rose-John S, Treiber M, Kloppel G, Yoshimura A, Reindl W, Sipos B, Akira S, Schmid RM, Algul H. Stat3/Socs3 activation by IL-6 transsignaling promotes progression of pancreatic intraepithelial neoplasia and development of pancreatic cancer. *Cancer cell.* 2011; 19:456–69. [PubMed: 21481788]
45. Bromberg J. Stat proteins and oncogenesis. *J Clin Invest.* 2002; 109:1139–42. [PubMed: 11994401]
46. Dougherty U, Sehdev A, Cerda S, Mustafi R, Little N, Yuan W, Jagadeeswaran S, Chumsangsri A, Delgado J, Tretiakova M, Joseph L, Hart J, Cohen EE, Aluri L, Fichera A, Bissonnette M. Epidermal growth factor receptor controls flat dysplastic aberrant crypt foci development and colon cancer progression in the rat azoxymethane model. *Clin Cancer Res.* 2008; 14:2253–62. [PubMed: 18413814]
47. Moser AR, Luongo C, Gould KA, McNeley MK, Shoemaker AR, Dove WF. ApcMin: a mouse model for intestinal and mammary tumorigenesis. *Eur J Cancer.* 1995; 31A:1061–4. [PubMed: 7576992]
48. Barker N, Ridgway RA, van Es JH, van de Wetering M, Begthel H, van den Born M, Danenberg E, Clarke AR, Sansom OJ, Clevers H. Crypt stem cells as the cells-of-origin of intestinal cancer. *Nature.* 2009; 457:608–11. [PubMed: 19092804]

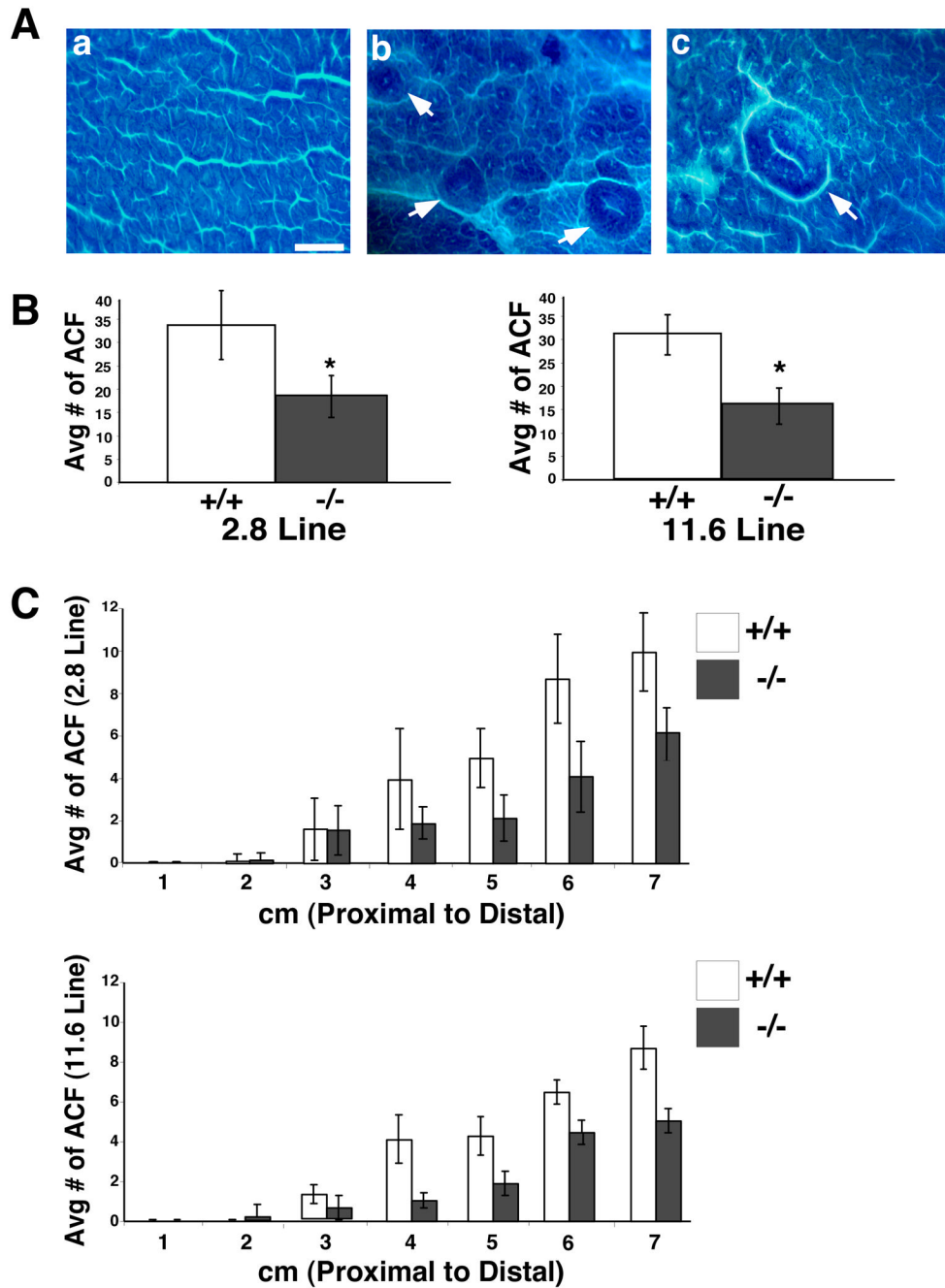


Figure 1.

Ptk6^{-/-} mice are resistant to AOM and develop fewer ACF. Wild type and *Ptk6*^{-/-} mice were subjected to six weekly injections of AOM and sacrificed 4 weeks after the last injection. Colons were stained with methylene blue. (A) Methylene blue stained colons of AOM treated wild type mice. (a) A region of stained normal colonic crypts. Size bar represents 500 μ m. (b) ACF (white arrows); (c) Magnified ACF involving multiple crypts and a slit-shaped luminal opening. (B) Total numbers of ACF were counted in *Ptk6*^{+/+} and *Ptk6*^{-/-} mice in two different *Ptk6*^{-/-} mouse lines (2.8 and 11.6). The increase in ACF in *Ptk6*^{+/+} mice is statistically significant (* $P < 0.05$, Bars \pm SD). (C) The average number of ACF across the length of the colon was recorded in two different *Ptk6*^{-/-} mouse lines.

Colons of *Ptk6* $+/+$ and *Ptk6* $-/-$ mice subjected to AOM were divided into 1 cm sections from the proximal to distal ends. The number of ACF that formed in each cm section was recorded for each mouse (Bars \pm SD).

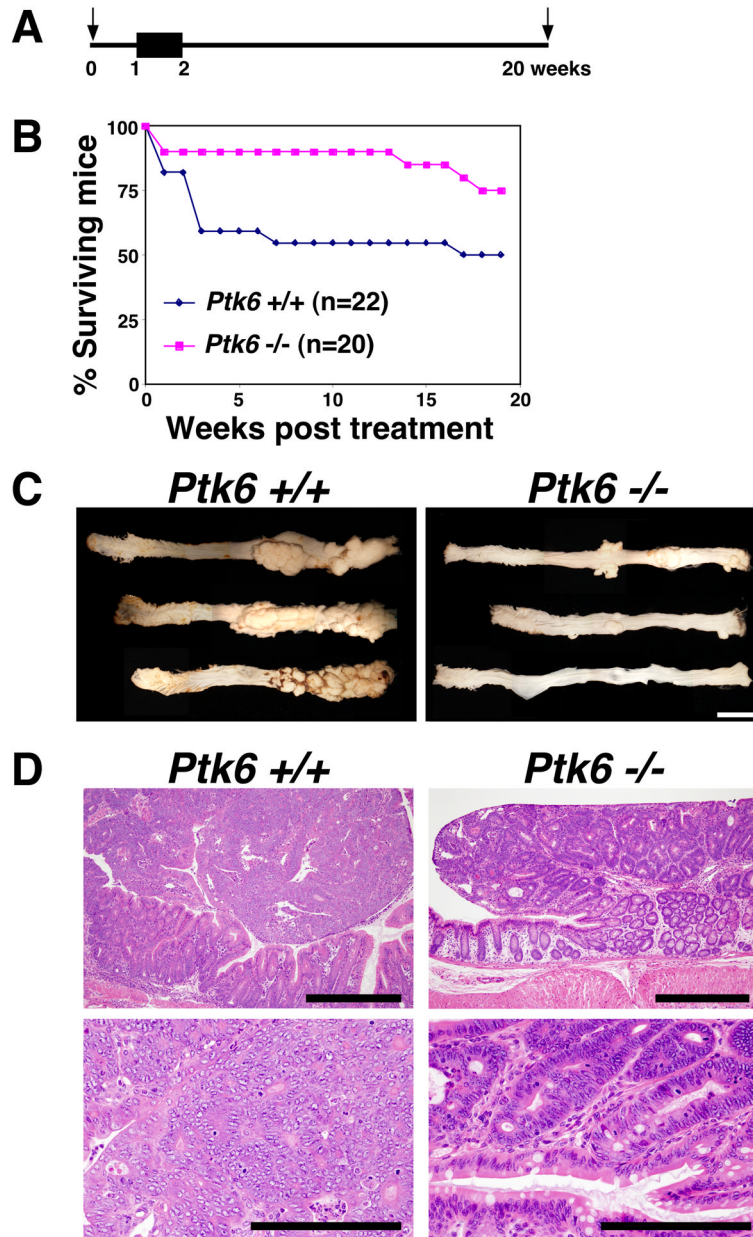


Figure 2.

$Ptk6^{-/-}$ mice are resistant to the AOM/DSS tumorigenesis protocol. (A) Wild type and $Ptk6^{-/-}$ mice were given a single injection of AOM, followed by one-week oral exposure to 2% DSS in drinking water. Arrows indicate the initial AOM injection at 0 weeks and the end of the study at 20 weeks. The black box indicates the 7 day treatment with 2% DSS. (B) The survival of $Ptk6^{+/+}$ and $Ptk6^{-/-}$ mice was monitored over the 20-week treatment period. A total of 22 wild type and 20 $Ptk6^{-/-}$ animals were examined. (C) At 20-weeks, $Ptk6^{+/+}$ and $Ptk6^{-/-}$ mice were sacrificed and their entire colons were excised and whole mounts were examined from proximal to distal ends using light microscopy. Increased numbers of nodular and polypoid colonic tumors were observed in colons of wild-type mice. Representative male $Ptk6^{+/+}$ and $Ptk6^{-/-}$ colons are shown. Size bars represent 1 cm. (D) Tumor sections were stained with hematoxylin and eosin. Pedunculated adenomas in $Ptk6^{+/+}$ mice had high-grade dysplastic cells with areas consistent with intramucosal

carcinoma, while low-grade dysplasia was seen in *Ptk6*^{-/-} mice. Size bars represent 500 μm (top) or 200 μm (bottom).

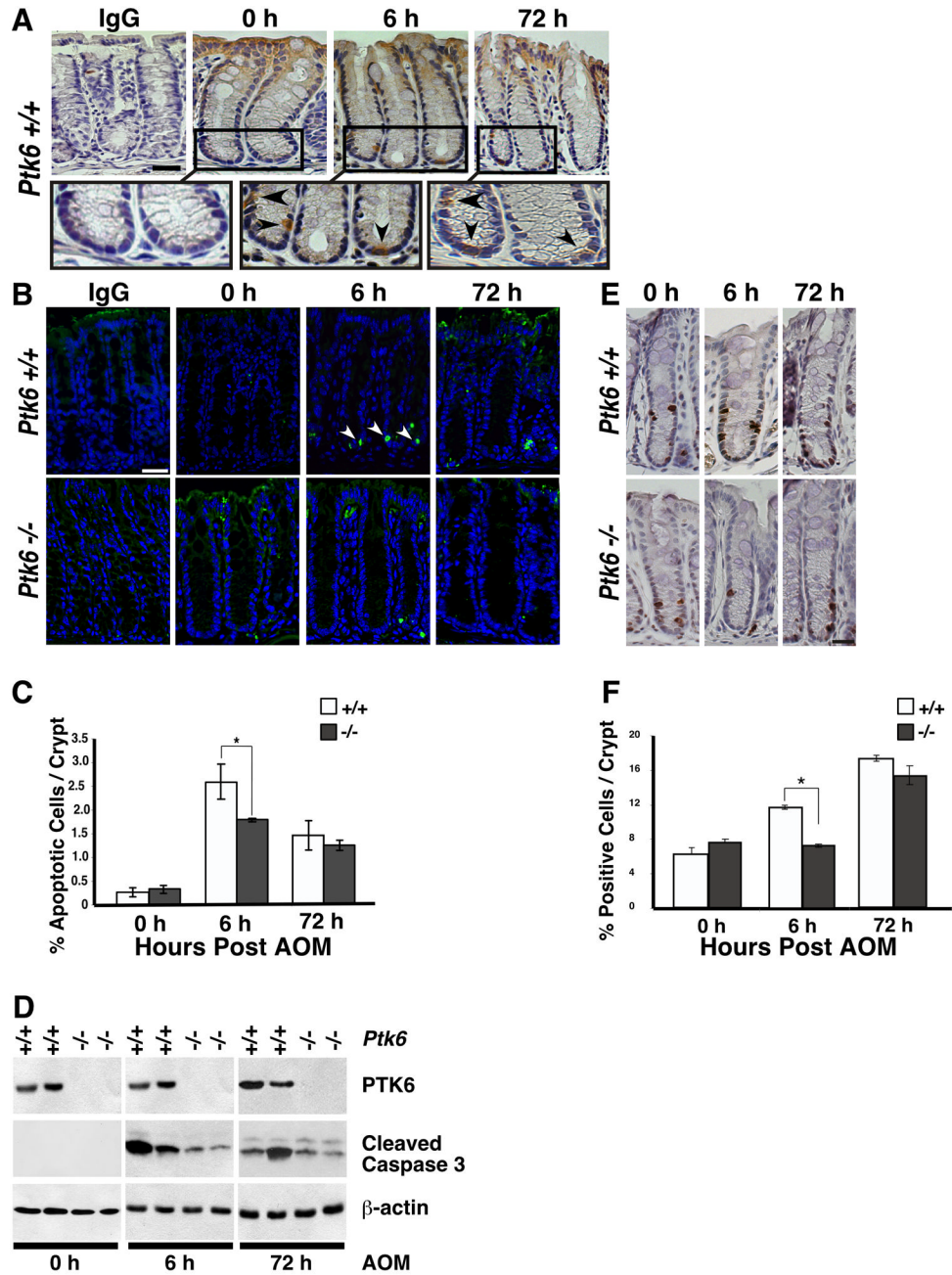
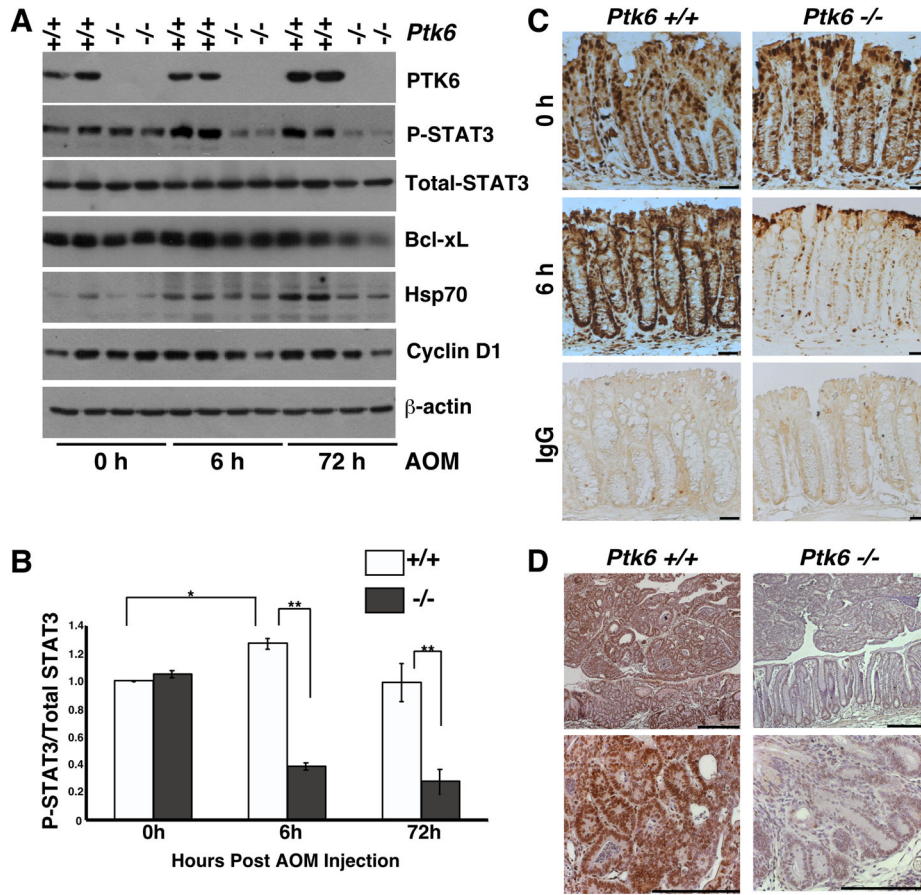


Figure 3. Induction of PTK6 in colonic crypts following AOM treatment correlates with increased apoptosis and proliferation. (A) PTK6 immunohistochemistry was performed on *Ptk6*^{+/+} colons at 6 or 72 hours after a single injection of AOM. Colon sections were counterstained with hematoxylin. The size bar represents 50 μm. Magnification of boxed areas (top panel) are shown below. Arrows denote PTK6 positive cells. (B) Cleaved Caspase-3 immunohistochemistry was performed on colon sections from *Ptk6*^{+/+} and *Ptk6*^{-/-} mice sacrificed at 6 or 72 hrs post AOM injection. Size bar represents 50 μm. (C) Cleaved Caspase-3 positive cells were counted in ten representative colonic crypts. Increased numbers of cleaved Caspase-3 positive cells were detected at 6 hours post AOM injection in *Ptk6*^{+/+} mice (* P < 0.05, Bars +/- SD). (D) Immunoblotting was performed with lysates

harvested at 6 or 72 hours post AOM injection, using antibodies directed against PTK6, cleaved Caspase-3, and β -actin. (E) BrdU immunohistochemistry was performed on *Ptk6*^{+/+} and *Ptk6*^{-/-} mice sacrificed at 6 or 72 hours post AOM injection. BrdU was injected 2 hours before animals were killed. (F) BrdU positive cells were counted in ten representative colonic crypts in *Ptk6*^{+/+} and *Ptk6*^{-/-} mice. The number of BrdU positive cells is higher in *Ptk6*^{+/+} mice (* P < 0.05, Bars +/- SD).

**Figure 4.**

PTK6 promotes STAT3 activation following AOM treatment. (A) Immunoblotting of lysates from *Ptk6*^{+/+} and *Ptk6*^{-/-} mice at 6 or 72 hours post AOM injection using antibodies directed against PTK6, activated P-STAT3 and total STAT3, Bcl-xL, Hsp70, Cyclin D1, and β actin. (B) The ratio of activated P-STAT3 over total STAT3 was quantified using NIH ImageJ and is represented as means \pm standard deviation (* P = 0.05; ** P = 0.02). (C) *Ptk6*^{+/+} and *Ptk6*^{-/-} mice were sacrificed 6 hours post AOM injection. Immunohistochemistry for P-STAT3 was performed. No counterstain was used and antibody binding was visualized using DAB (brown). Size bar represents 50 μ m. IgG staining serves as a negative control. (D) P-STAT3 immunohistochemistry was performed with sections from tumors that formed in *Ptk6*^{+/+} and *Ptk6*^{-/-} mice exposed to AOM/DSS (Figure 2D). Size bars represent 100 μ m. Sections were counterstained with hematoxylin and antibody binding was visualized using DAB.

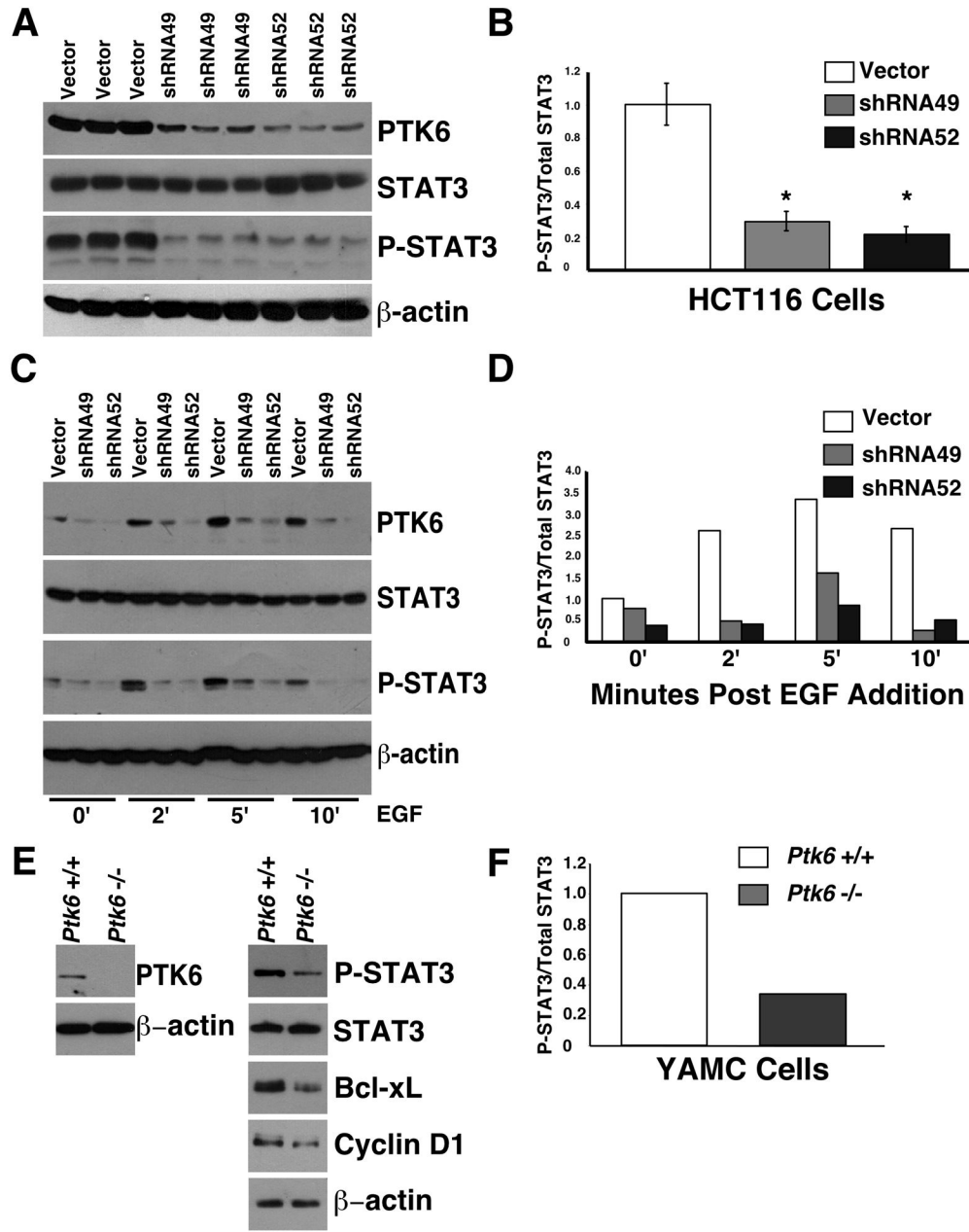


Figure 5. PTK6 regulates STAT3 activation in human and mouse colon cell lines. (A) Immunoblot analysis of lysates prepared from HCT116 cell lines containing empty vector or two different PTK6 shRNA's (shRNA49, shRNA52). (B) The ratio of P-STAT3 over total STAT3 is represented as means \pm standard deviation (* $P = 0.002$). (C) HCT116 cells expressing empty vector, shRNA49 or shRNA52 were serum starved and stimulated with EGF for 2, 5 or 10 minutes. Immunoblotting was performed using antibodies against PTK6, P-STAT3, total STAT3, and β -actin. (D) The ratio of P-STAT3 over the total STAT3 band density following EGF treatment was quantified using NIH ImageJ. (E) Immunoblot analysis of lysates from wild type YAMC cells and *Ptk6*^{-/-} YAMC cells. (F) The ratio of P-STAT3 over the total STAT3 is shown.